Journal of Physics: Conference Series

**PAPER** • **OPEN ACCESS**

# Investigation of noise reduction effects of individual and combined geometrical modifications on UAM propeller blades

To cite this article: D Skrna *et al* 2024 *J. Phys.: Conf. Ser.* **2716** 012060

# Investigation of noise reduction effects of individual and combined geometrical modifications on UAM propeller blades

D Skrna, M de Rosa Jacinto da Silva, M Berens

Technische Universität Wien, Research Group Aircraft Systems E307-02-2, Lehárgasse 6, 1060 Vienna, Austria

E-mail: dominik.skrna@tuwien.ac.at

**Abstract.** The development of a future transportation concept in cities may also include transportation of passenger and cargo at various altitudes in order to reduce the load on the ground infrastructure. This is known as urban air mobility (UAM), facilitated by the application of electrical vertical take-off and landing (eVTOL) vehicles. Public acceptance is required with regard to safety aspects in densely populated areas, but also in terms of noise emissions. As with almost any aircraft, the propulsion systems, in most cases the propeller blades, are the main source of noise generation. In literature, experimental and numerical results for geometric blade modifications for the purpose of noise reduction are provided only for small diameter propellers. This paper investigates the individual features at larger diameter propellers by means of numeric aeroacoustic simulations with OpenFOAM. The modifications include serrations of the trailing edge, leading edge tubercles and blade tip adaptations. Moreover, the combination of those features is investigated in a parameter study for various rotational velocities and several flight modes. The key effect, namely a reduction of broadband noise, can be observed for several cases, but the strength of it varies. An optimization process is necessary to obtain an efficient noise reduction for all operating conditions of a particular aircraft design.

**Keywords: UAM, propeller noise, noise reduction, serration, tubercles**

## 1. Introduction

The development of aircraft that can be used in urban areas and expand urban mobility differs significantly from helicopters that have been used so far. Depending on the size of these eVTOL vehicles, both people and goods are expected to be transported in cities in the future without being tied to the ground level. Especially due to the application in densely populated areas, correspondingly high safety requirements must be met. This promotes the social acceptance of these aircraft, together with the reduction of noise emissions. Consequently, it is necessary to overcome major preconceptions, which include the clear perception of aircraft passing by at low altitude during take-off, climb, approach and landing, especially due to sound reflections in densely built-up cities. Not only the human well-being depends on noise reduction technologies, but the environment also needs to be protected from excessive noise pollution. Therefore, the possibilities of geometry-based noise reduction of propeller blades used for urban air mobility vehicles has received significant research attention. Most of those studies have focused mainly on one individual feature, therefore this paper aims to investigate the combination of several geometrical modifications simultaneously. The computational aeroacoustic simulations of this paper focus on the vertical operational phases, namely climb and hovering as well as descent, of such aircraft. This paper is based on the results of the diploma thesis of the author [1].

## 2. Propeller geometrical design modifications

The influence of additional geometrical modifications on the aerodynamic and aeroacoustic behaviour of propeller blades according to literature research is summarized in this chapter. The optimized propeller geometry concept of this paper is discussed in chapter 4 and 5. As the described effects are based on studies of small propellers with a diameter of up to 0,3 m, a deviation of the strength of the effects cannot be excluded for larger propeller diameters.

### *2.1. Fundamental geometry parameters*

Already the basic geometrical design parameters of propellers, such as blade sweep, thickness to chord ratio, pitch angle, twist, number of blades as well as propeller diameter and airfoil shape have a significant influence on the aerodynamic and aeroacoustic behaviour [2]. The increase of the pitch value for example is associated with increased thrust and a higher SPL output at the same rotational velocity [3]. The thickness ratio can contribute to the harmonic noise as a thickness noise source, which is proportional to the volume of air that is displaced by the rotating propeller blade [4]. The results of [5] indicate that the aerodynamic efficiency is not affected by the blade sweep angle, even for very high sweep values. In terms of aeroacoustics, sweep can reduce monopole noise sources for specific directivity angles. The blade sweep causes a shift of the loading noise to radial positions closer to the hub, where lower Mach numbers occur. The strength of the effect depends on the rotational velocity [6].

### *2.2. Additional geometrical modifications*

The bio-inspired adaptation of the trailing edge, which can be seen primarily by looking at the wings of birds, is a recently intensively researched topic. The modification options range from the radial positioning to the geometric shape as well as number and depth of the serrations [7]. The main effect of the serration of the trailing edge is the change of the flow structure that passes the airfoil. Due to the different chord lengths depending on the radial position, the resulting pressure distribution leads to a reorientation of the vortices which, together with the turbulent boundary layer, improves the mixing process of the upper and lower flow alongside the airfoil. The resulting redistribution of momentum and turbulent shear stress close to the serration edges leads to an improved aeroacoustic behaviour [8]. In general, a reduction of the broadband noise in the high frequency range can be determined when comparing untreated trailing edges with serrated ones. Serrations over the entire span have not proven to be useful because modifications in the tip region have a greater influence than at the blade`s root [9].

Protuberances of the leading edge, also called tubercles, are a geometric adaptation whose origin can again be found in nature, for instance on the fins of whales. Their influence is visible in the delay and the reduction of the effects of boundary layer separation. Like for the serrated trailing edge, the radial position as well as the size and depth of the tubercles play a decisive role for the aerodynamic and aeroacoustic output [10].

The tip vortices also contribute largely to the noise generated by the propeller and are therefore part of the optimization process. There are many different concepts for blade tip modifications studied in literature: anhedral/dihedral winglets, Ogee tips, oval tips [4] as well as trailing edge notches and vortex generators [11]. Although there are no aeroacoustic studies available regarding swept back anhedral tips, it was decided to investigate the effects of this modification in this work along with the addition of a trailing edge notch. There are two vortices generated close to the blade tip, one at the notch and one at the blade tip. Both vortices coalesce after a short time which leads to a dissipation of them and results in a reduction of the strength of the tip vortex as well as its influence downstream [11].

## 3. Propeller modelling, meshing process and CFD simulation setup

The propeller blade geometry can be characterized by several parameters at multiple radial positions. Typically, only the relative chord length and the pitch angles are specified, but for the generation of the geometry for this paper, the offset to the reference line was also necessary. This parameter can be calculated using the mid-chord alignment values. By knowing those quantities as well as the applied airfoils at several radial positions, the geometry of the propeller blade can be determined.

By running a Python script provided by [12], the points and splines of the blade cross-sections as well as the trailing and leading edge guidance lines can be obtained from the input parameters and the airfoil datasets. This simplifies the import in CATIA. The Python script also offers the opportunity to interpolate between several airfoils at different radial positions. The APC 27x13E propeller of the company Advanced Precision Composites (APC) Propellers, which is commercially available, was selected as the reference propeller. Detailed geometry data are not listed here because they are available from the manufacturer [13]. A comparison of the recreated version of this propeller in CATIA and the original one is displayed in figure 1. The applied airfoils are E63 ($0{,}26 \leq r/R < 0{,}57$) and NACA 4412 ($0{,}57 \leq r/R < 1$) as given by APC. For the connection to the hub, a NACA 4430 airfoil was selected because of the increased thickness value.

**Figure 1.** APC 27x13E original (left) [13], recreation in CATIA (right)

The meshing was carried out in OpenFOAM by using the software integrated meshing tools “blockMesh” and “snappyHexMesh”. Several levels of refinement are applied to ensure an accurate representation of the individual geometric features. Special attention must also be paid to the transition from the rotating cylinder to the static mesh. Furthermore, an external acoustic library was implemented in OpenFOAM for near and far-field noise computation. It contains three prediction models for acoustic noise, of which the Ffowcs-Williams-Hawkings (FWH) analogy [14] is useful for the given simulation setup. The frequencies and corresponding SPL values are calculated at the specified observer positions. Due to the given analogy with the corresponding control surface, a larger computational effort can be avoided, since the observers do not have to be located within the mesh [15]. Figure 2 shows the simulation setup and corresponding geometry data. The small red cylinder represents the rotating cylinder, which includes the propeller geometry. The large blue cylinder represents the FWH control surface, that is opened on the side of the wake region of the propeller (dashed line) following the recommendations of [16]. The rotation of the propeller is in the direction of the negative y axis according to the right-hand rule.

For the acoustic simulations, microphones are positioned at every 5° on the perimeter of the rotational plane (xz in blue) and the plane transverse to it (yz in red) at a distance of 5 m to the noise source (see figure 3). For the yz plane, there are no data in the wake behind the propeller because of reduced accuracies due to the chosen FHW control surface set-up.

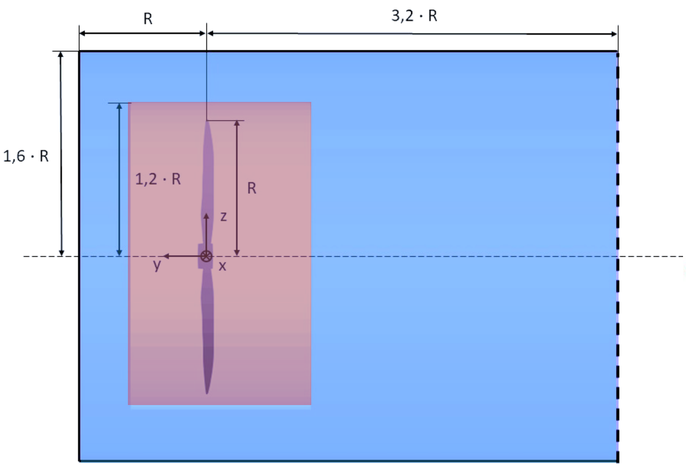


**Figure 2.** Simulation set-up: dynamic cylinder (red), FWH control surface (blue)

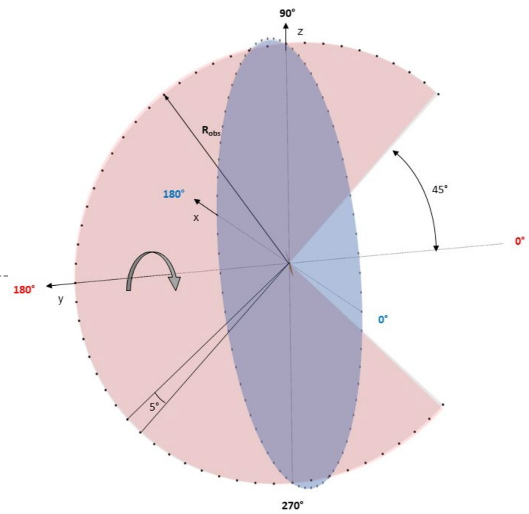


**Figure 3.** Microphone positions in two planes

The computationally demanding simulations were carried out using the Vienna Scientific Cluster (VSC) supercomputer infrastructure. A Reynolds Averaged Navier-Stokes (RANS) turbulence model for the incompressible flow was selected due to the several different applied scales, especially with regard to the mesh sizes. The validation of this OpenFOAM model was conducted using literature data for propeller diameters of up to 30 cm. A mesh quality study was performed and concluded that about two million cells are sufficient enough for a high quality simulation output.

## 4. Individual geometrical modifications on larger propeller diameter

In this chapter the effects of the application of individual geometrical modifications on the given reference propeller by APC are investigated. A rotational velocity of 5000 RPM and an advance ratio of 0,1 were selected, which represents climbing with an inflow velocity of 5,75 m/s. The individual geometrical modifications are described in more detail in the corresponding subchapters. Table 1 summarized the aerodynamic results for all the investigated cases.
For better comparability, the 1/12 octave band SPL output was also plotted for frequencies higher than 1000 Hz. In that way, the broadband noise can be better compared. Furthermore, the directivity patterns are also plotted for the first three blade passing frequencies (BPF) and the OASPL value. Those graphs give information about the character of the noise source.

**Table 1.** Summary of the thrust and required power output for each simulation case.

| | Thrust (N) | Power (W) |
|---|---|---|
| **Reference case** | 133 | 2997 |
| **LE tubercles** | 133,1 | 3029 |
| **TE serration** | | |
| 4820 RPM | 133,8 | 2940 |
| 5000 RPM | 143 | 3298 |
| **Tip modification** | | |
| No notch | 133,9 | 3059 |
| With notch | 132,9 | 3016 |

### *4.1. Leading edge tubercles*

The radial positioning (0,75 ≤ r/R < 0,95) as well as size of those tubercles (see figure 8) were selected according to the results of a literature research. The SPL output between the tonal noise peaks, which is associated with narrow band random noise, is lower than the one of the reference geometry. The 1/12 octave band results in figure 4 indicate local SPL reductions of up to 5 dB especially between 1000 Hz and 2000 Hz. As described by [10], a change of the directivity pattern is visible.

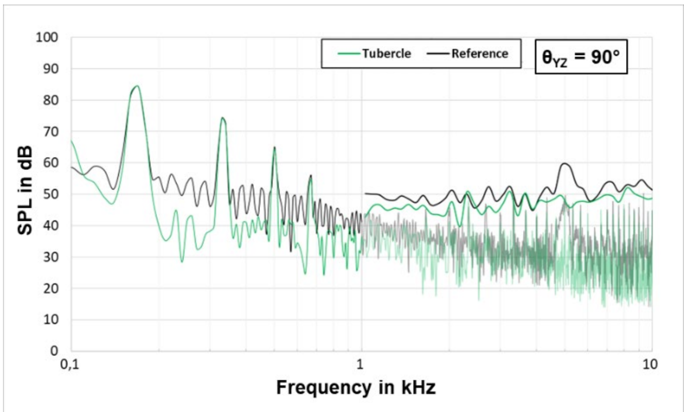


**Figure 4.** SPL output plotted over frequency for the leading-edge tubercles (green), unmodified case (black)

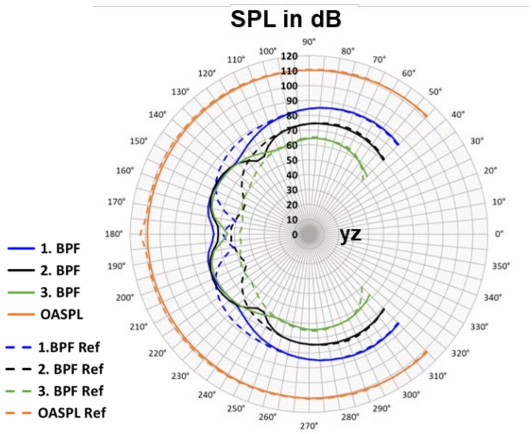


**Figure 5.** Directivity pattern in the yz plane for BPFs and OASPL output

Especially in front of the propeller between 135° and 225°, an almost constant SPL distribution for the modified propeller is visible for all three displayed blade passing frequencies. In comparison to the output of the reference propeller, which is visualized with dashed lines, this leads to locally higher SPL values for all BPFs. The reason for this is assumed to be the greater level of loading noise. Responsible for this are the pressure values, which are higher in magnitude and located radially further inwards, which contributes to a local amplification effect of the dipole source. On the other hand, the differences to the reference propeller in the xz plane are small for all BPFs and the OASPL values.

### *4.2. Trailing edge serrations*

Serrations with a constant wavelength and amplitude were added to the trailing edge (0,35 ≤ r/R < 0,95) yielding an increase of the blade planform area. This results in a higher thrust value at the baseline rotational velocity of 5000 RPM. The required power increases significantly. Nevertheless, there is already a reduction of the broadband noise noticeable for this case at the unchanged RPM value (see red line in figure 6). As it is an objective of this work to keep the generated thrust constant, the rotational velocity was reduced to 4820 RPM. This has not only led to the generation of a comparable thrust, but also to a reduction of the required power by 2%. In terms of aeroacoustics, the reduced rotational velocity (see figure 6 orange line) indicates minor decibel reductions at the tonal noise peaks. Due to the change of the rotational velocity, the blade passing frequency also decreases which is the reason for the shifted peaks in this simulation output. Both serration cases result in roughly the same broadband noise reduction. The directivity plots indicate that there are only small changes of the SPL output for both RPM cases in comparison to the unmodified case. Furthermore, the OASPL values are slightly higher for the case with the reduced RPM value. The investigated cases show the potential of geometric optimization, which not only leads to acoustic improvements, but can also achieve power reductions while maintaining the same thrust.

### *4.3. Blade tip modifications*

The last individual geometrical modification described in this paper are blade tip modifications (0,95 ≤ r/R < 1). It was decided to change the given blade geometry to a swept back anhedral tip. Additionally, a notch was added close to the tip due to the promising results from literature. The consistency of the thrust, the almost equal required mechanical power, as already stated in table 1, and the reduced SPL output favor the implementation of the notch. The tip with the notch results in an even further reduction of the narrow band random as well as broadband noise, related to the tip modification without notch. This is clearly indicated by the 1/12 octave band results, which show a decibel reduction of about 10 dB between 1000 and 1500 Hz (see figure 7). However, also for this modification, the tonal noise peaks at the blade passing frequencies remain unchanged. The analysis of the directivity patterns for the small tip and the same tip with notch, show minimal deviations from each other. A study to determine the influence of blade tip sweep angle and anhedral angle on the aerodynamic and aeroacoustic behaviour of propellers of this size is necessary for further improvement of the results.

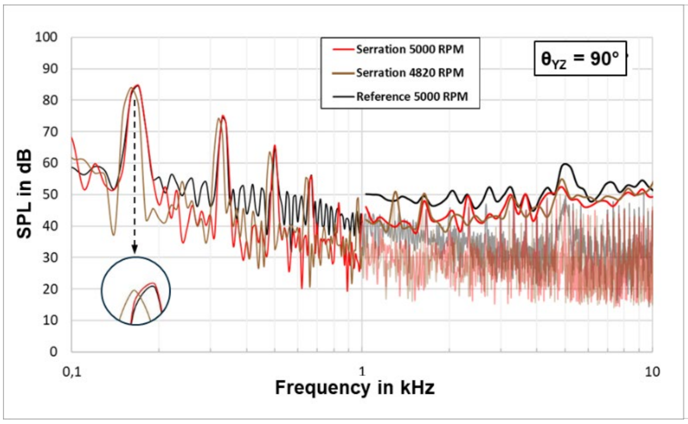


**Figure 6.** SPL output plotted over frequency for trailing-edge serrations (red, brown), unmodified case (black)

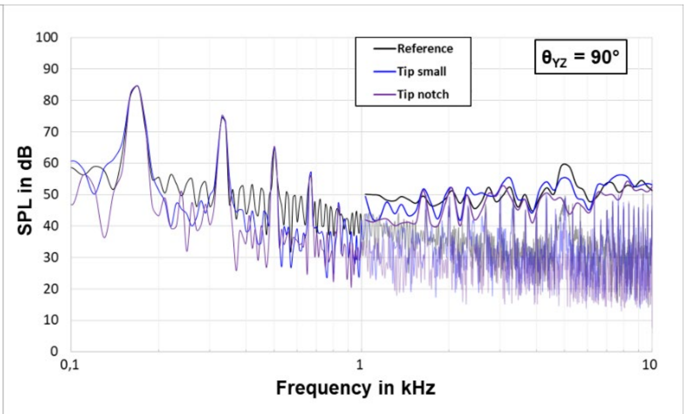


**Figure 7.** SPL output plotted over frequency for the tip modifications (blue, purple), unmodified case (black)

## 5. Combination of several geometrical modifications

The modifications described in chapter 4 are combined in this part of the paper (see figure 8). Once again it has to be stated that the geometry of those features is based on the results of a literature research for smaller diameter sizes. Therefore, an optimization process regarding all modifications is necessary. As the time averaged thrust is just slightly higher than in the reference case (about 1%), no adaptation of the rotational velocity is carried out. This also simplifies the comparability of the data in the parameter study. It can be noted that the large thrust increase of the serrations is no longer present when combining the modifications. Approximately 5% more power is required to obtain the desired RPM value than for the unmodified reference propeller. The decrease of the narrow band random noise and sections of the broadband noise, which are also partially observed in the simulations of individual features, are preserved for an observer in the rotational plane (see figure 9).

**Figure 8.** Geometry of the combination case with all individual modifications applied

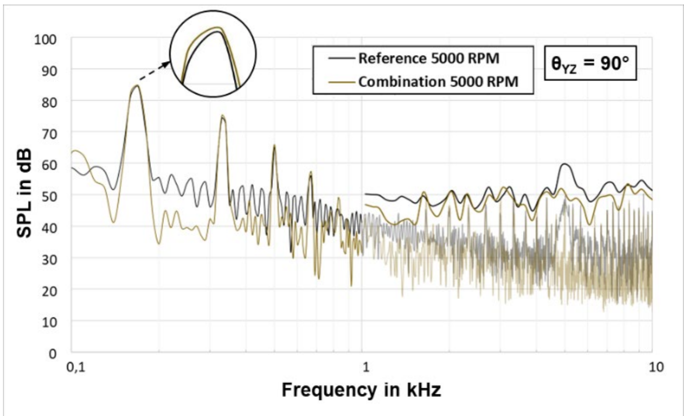


**Figure 9.** SPL output plotted over frequency for the combination case (gold), unmodified case (black)

## 6. Parameter study

The parameter study was divided in two sections, in which the flight mode as well as the rotational velocity are changed separately. Propeller blade pitch adjustments can practically be performed utilizing a swash plate as it is applied in most helicopters. For small and medium size UAM's the complexity of swash plates is avoided, and propeller thrust is solely adjusted by modulation of the rotational speed. However, for computational purposes the advance ratio, which is linked to the inflow velocity, needs to be changed. Therefore, for hovering the advance ratio was set to zero and descending can be simulated by selecting a negative advance ratio. It is difficult to predict the output of those simulations as there are only a few sources available in literature for negative advance ratio propeller simulations. Furthermore, so called vortex ring state effects must be taken into account, which describe the recirculation of the flows from the wake region of the propeller.

In the second part of the study, the rotational speed for the climb case was changed. Simulations were carried out for 3000, 4000, 6000 and 7000 RPM and are compared to the initial 5000 RPM case. Along with the expected change of the BPFs, differences in the broadband noise output can be seen as well. Regarding the generated thrust, only a small deviation between the reference propeller and the geometry with all modifications combined can be seen for all considered rotational velocities for the climb operation (see figure 10 green lines). On the contrary, with regard to the required mechanical power to achieve the corresponding rotational speeds, a clear deviation between the two geometries occurs. An increase in the required power for the combination case in relation to the reference case with increasing rotational velocity is visible (see figure 10 blue lines).

The collected results of this parametric study in terms of OASPL, as well as the evaluations of the different flight modes from the previous chapter, are shown in figure 11 for an observer at $\theta = 90°$. The outputs of the simulations based on the reference geometry (squares) and the ones of the propeller with all combined modifications (triangles) are displayed. For the climb case, for which results are available at several rotational velocities, a clear trend of the OASPL data can be seen. For low RPM values, the overall sound pressure level is clearly lower for the combined geometry than for the unmodified one. There is a transition point at 5200 RPM, where this behaviour changes to the opposite. These conclusions are relevant for further studies on the optimization of the influence of geometrical features on the acoustic behaviour. With regard to the other two flight modes, statements are only possible for a rotational velocity of 5000 RPM. The geometric modifications are advantageous during hovering, but disadvantageous for the descent flight case. However, it still must be considered that these are only the OASPL values and that this does not allow any conclusions to be drawn about the tonal noise peaks or the broadband noise development. For that, as in the previous chapters, the individual frequency spectra must be assessed.

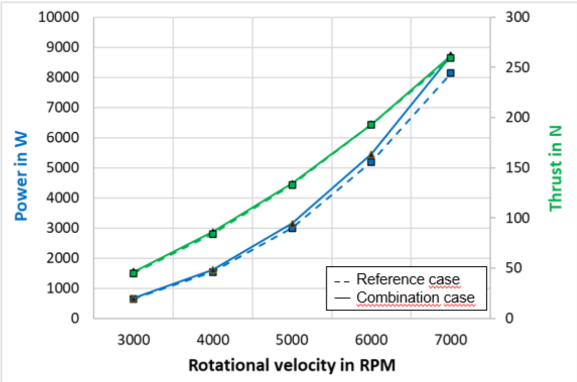


**Figure 10.** Thrust (green) and power (blue) comparison for the combination and the unmodified geometry case

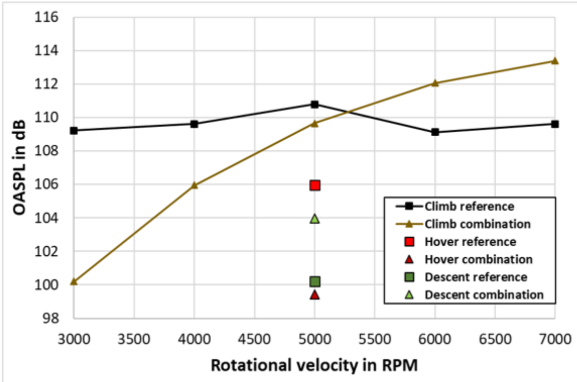


**Figure 11.** OASPL plotted for several RPM values of the combination case and the unmodified geometry case

## 7. Conclusion and outlook

Within the scope of this paper, numerous simulations were carried out using the CFD software OpenFOAM in order to analyze the aerodynamic and aeroacoustic behaviour of different propeller geometries. Since only aeroacoustic results for small propeller diameters are available in literature, the individual geometric features, namely leading edge tubercles, trailing edge serration and blade tip modifications, for a propeller with a diameter of 0,69 m had to be simulated first. The application of those modifications on larger propeller diameters can also lead to a noise reduction effect, however, it is important to study the effects of those features referred to the diameter size in order to better select the corresponding parameters.

In the second part of this paper, the investigated modifications were combined on one propeller blade. for climb, hover and descent cases at 5000 RPM. Concerning the climb case, a significant reduction of the broadband noise of up to 8 dB below 1500 Hz and above 5000 Hz can be seen. However, the tonal noise peaks are hardly changed compared to the reference. The hover and descent flight mode results lead to an increased broadband noise in relation to the reference geometry, however, there is a general decrease of the OASPL output value for the investigated rotational velocity. The combination of geometric modifications leads to a noise reduction in the hover case in comparison to the results of the reference geometry in that flight mode, while the opposite is observed for the descent flight case.

The results of the OpenFOAM simulations of this paper indicate that a potential for noise minimization is given by combining several geometrical modifications. The perspective for optimization in terms of aerodynamic and aeroacoustic properties through the application of geometric modifications is very promising. Therefore, it is even more important to find a trade-off between rotational velocity, advance ratio, required power, generated thrust and diameter of the propeller in combination with the targeted application of geometrical adjustments. The addition of horizontal flight modes in combination with the vertical ones is a field of future research.

**Acknowledgments**
The research presented in this publication has been conducted by the Research Group for Aircraft Systems of TU Wien. The Research Group receives funding from the Austrian Aviation Programme TAKE OFF via the BMK Endowed Professorship for Innovative Aviation Technologies.

## 8. References

[1] Skrna D 2023 Combined propeller blade geometrical modifications to reduce noise emissions of urban air mobility vehicles *Diploma Thesis* Technische Universität Wien, https://doi.org/10.34726/hss.2023.112808
[2] Hubbard H 1991 Aeroacoustics of Flight Vehicles: Theory and Practice *NASA Reference Publication* 1: 1 – 64, https://ntrs.nasa.gov/citations/19920001380
[3] Pang E, Cambray A, Rezgui D, Azarpeyvand M and Showkat Ali S 2018 Investigation Towards a Better Understanding of Noise Generation from UAV Propellers *AIAA/CEAS Aeroacoustics Conference* AIAA 2018-3450, https://doi.org/10.2514/6.2018-3450
[4] Henricks Q 2019 Computational Aerodynamic and Aeroacoustic Study of Small-Scale Rotor Geometries *Master's thesis* Ohio State University, http://rave.ohiolink.edu/etdc/view?acc_num=osu1546618814905583
[5] Wiedemann A 2020 A Study of the Aeroacoustics of Swept Propellers for Small Unmanned Aerial Vehicles *Master thesis* Old Dominion University, https://doi.org/10.25777/8qwv-vq29
[6] de Haan W 2021 Impact of Blade Sweep on Aerodynamic and Aeroacoustic Performance Optimization of Isolated Propellers *Master thesis* Delft University of Technology, http://resolver.tudelft.nl/uuid:09137b04-f499-47f5-9c17-7334d0ef92ac
[7] Wei Y, Qian Y, Bian S, Xu F and Kong D 2021 Experimental Study of the Performance of a Propeller with Trailing-Edge Serrations *Acoustics Australia* **49**: 305 – 16, https://doi.org/10.1007/s40857-021-00221-w
[8] Chong T and Vathylakis A 2015 On the aeroacoustic and flow structures developed on a flat plate with a serrated sawtooth trailing edge *Journal of Sound and Vibration* **354**: 65 – 90, https://doi.org/10.1016/j.jsv.2015.05.019
[9] Ning Z, Wlezien R and Hu H 2017 An Experimental Study on Small UAV Propellers with Serrated Trailing Edges *AIAA Fluid Dynamics Conference* 3813, https://doi.org/10.2514/6.2017-3813
[10] Asghar A, Perez R, Jansen P and Allan W 2020 Application of Leading-Edge Tubercles to Enhance Propeller Performance. *AIAA Journal* **58**: 4659 – 71, https://doi.org/10.2514/1.J058740
[11] Treuren K and Wisniewski C 2019 Testing Propeller Tip Modifications to Reduce Acoustic Noise Generation on a Quadcopter Propeller *ASME Journal of Engineering for Gas Turbines and Power* 141(12), https://doi.org/10.1115/1.4044971
[12] De Rosa Jacinto M 2021 Aerodynamic Effect of a Wingtip - Mounted Propeller *Diploma Thesis* University of Sao Paulo
[13] Advanced Precision Composites (APC) Propeller, https://www.apcprop.com/
[14] Ffowcs Williams J and Hawkings D 1969 Sound Generation by Turbulence and Surfaces in Arbitrary Motion. *Philosophical Transactions of the Royal Society of London. Series A, Mathematical and Physical Sciences* **264**: 321 – 42, https://doi.org/10.1098/rsta.1969.0031
[15] Epikhin A, Evdokimov I, Kraposhin M, Kalugin M and Strijhak S 2015 Development of a Dynamic Library for Computational Aeroacoustics Applications Using the OpenFOAM Open Source Package *Proc. Comp. Sci.* **66**: 150 – 57, https://doi.org/10.1016/j.procs.2015.11.018
[16] Afari S 2019 Prediction of Noise Associated with an Isolated UAV Propeller *Doctoral Dissertations and Master's Theses* 463, https://commons.erau.edu/edt/463